

Yannick Bourgat | Brigitte Tiersch | Joachim Koetz | Henning Menzel

Enzyme degradable polymersomes from Chitosan-g-[poly-l-lysine-block-epsilon-caprolactone] copolymer

Suggested citation referring to the original publication:

Macromolecular bioscience 21 (2020) 1, Art. 2000259 pp. 1 - 9

DOI <https://doi.org/10.1002/mabi.202000259>

ISSN 1616-5187, 1616-5195

Journal article | Version of record

Secondary publication archived on the Publication Server of the University of Potsdam:

Zweitveröffentlichungen der Universität Potsdam : Mathematisch-Naturwissenschaftliche Reihe 1382

ISSN: 1866-8372

<https://nbn-resolving.org/urn:nbn:de:koby:517-opus4-566584>

DOI: <https://doi.org/10.25932/publishup-56658>

Terms of use:

This work is licensed under a Creative Commons License. This does not apply to quoted content from other authors. To view a copy of this license visit

<https://creativecommons.org/licenses/by/4.0/>.



Enzyme Degradable Polymersomes from Chitosan-*g*-[poly-L-lysine-*block-ε*-caprolactone] Copolymer

Yannick Bourgat, Brigitte Tiersch, Joachim Koetz, and Henning Menzel*

The scope of this study includes the synthesis of chitosan-*g*-[peptide-poly- ϵ -caprolactone] and its self-assembly into polymeric vesicles employing the solvent shift method. In this way, well-defined core-shell structures suitable for encapsulation of drugs are generated. The hydrophobic polycaprolactone side-chain and the hydrophilic chitosan backbone are linked via an enzyme-cleavable peptide. The synthetic route involves the functionalization of chitosan with maleimide groups and the preparation of polycaprolactone with alkyne end-groups. A peptide functionalized with a thiol group on one side and an azide group on the other side is prepared. Thiol-ene click-chemistry and azide-alkyne Huisgen cycloaddition are then used to link the chitosan and poly- ϵ -caprolactone chains, respectively, with this peptide. For a preliminary study, poly-L-lysine is a readily available and cleavable peptide that is introduced to investigate the feasibility of the system. The size and shape of the polymersomes are studied by dynamic light scattering and cryo-scanning electron microscopy. Furthermore, degradability is studied by incubating the polymersomes with two enzymes, trypsin and chitosanase. A dispersion of polymersomes is used to coat titanium plates and to further test the stability against enzymatic degradation.

hydrophilic and hydrophobic drugs with a high encapsulation efficiency.^[3,4] This parameter is one of the most important factors for any drug delivery system (DDS). For instance, DDS with low encapsulation efficiency would require a higher quantity of polymeric materials to achieve the appropriate drug concentration and can lead to a stronger immune response.^[3] Besides polymersomes were proven to be more stable and less water-permeable compared to liposomes like phospholipid vesicles.^[1] Indeed, liposomes have been described as leaky structures with poor retention efficiencies. On the other hand, polymersomes offer the possibility to control the diffusion rate by varying the amount/length of the hydrophobic segment.^[5,6] Moreover, natural and synthetic lipids cannot easily be functionalized. Even small modifications at the head group can have a significant impact on the properties and thus on the self-assembly into liposomes. On the other hand modification of the lipid tail(s) requires often

1. Introduction

Over the past years, self-assembled polymeric systems have been suggested for many applications. Amphiphilic graft-copolymers, composed of hydrophobic and hydrophilic segments, are able to self-assemble into core-shell nanostructured systems with tunable size, so called polymersomes.^[1,2] Polymersomes have become interesting carriers, which can encapsulate both

several synthetic steps. On the contrary, polymersomes surface-functionalization can be achieved by using polymers that carry functional groups on their chains.^[1] For example Amos et al. prepared polymersomes with surface azide groups and functionalized them with dendritic polyesters without affecting the stability of the structure.^[7] Finally, they are capable of structural and chemical changes in response to various endogenous as well as exogenous stimuli such as pH,^[8] temperature,^[9] redox-potential,^[10] electric fields,^[11] magnetic fields,^[12] and enzymes^[13] to trigger cargo release.

Due to the overexpression of enzymes involved in pathological conditions, enzyme responsive DDS are an interesting approach in the field of infection and cancer therapies. Since enzyme responsiveness can result in very high selectivity toward specific targets, they would also offer a broad range of new and innovative applications. To prepare enzyme responsive DDS the substrate of the enzyme has to be integrated into the polymer which forms the DDS. For instance, peptides cleavable by enzymes can be introduced and their cleavage destabilizes the nanocarrier structure resulting in a release of encapsulated drugs. If the enzyme is secreted in the diseased tissue, the drug would be released only there. Law et al. have developed such a drug delivery system based on peptides.^[14] In aqueous solution, the system self-assembled into a gel scaffold. Treatment with appropriate protease led to cleavage of the peptide

Y. Bourgat, Prof. H. Menzel
 Technische Universität Braunschweig
 Institute for Technical Chemistry
 Hagenring 30, 38106 Braunschweig, Germany
 E-mail: h.menzel@tu-braunschweig.de

Dr. B. Tiersch, Prof. J. Koetz
 Universität Potsdam
 Institute of Chemistry
 Karl-Liebknecht Str. 24-25, 14476 Potsdam, Germany

The ORCID identification number(s) for the author(s) of this article can be found under <https://doi.org/10.1002/mabi.202000259>.

© 2020 The Authors. Macromolecular Bioscience published by Wiley-VCH GmbH. This is an open access article under the terms of the Creative Commons Attribution-NonCommercial License, which permits use, distribution and reproduction in any medium, provided the original work is properly cited and is not used for commercial purposes.

DOI: 10.1002/mabi.202000259

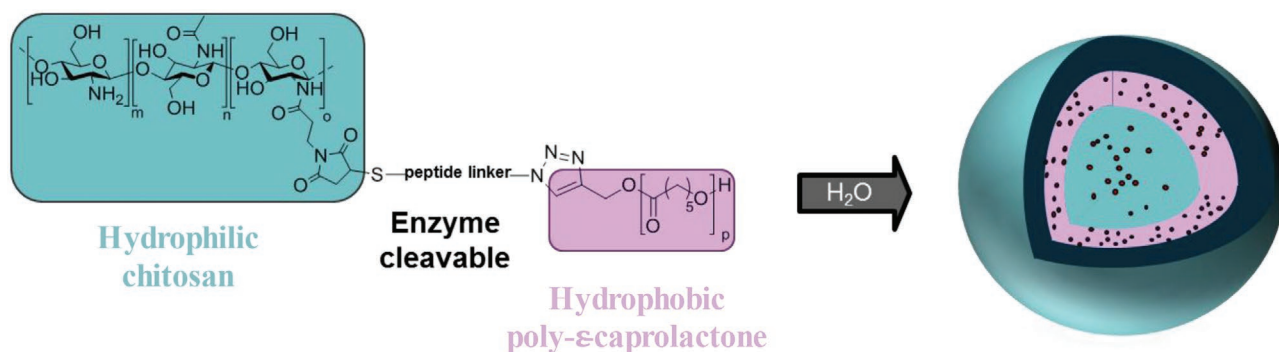


Figure 1. Schematic representation of Chitosan-g-[PLL-poly- ϵ -caprolactone] copolymer and polymersome.

and, subsequently to the degradation of the gel.^[14] Tolle et al. prepared an aggrecanase-labile peptide sequence combined with spacers (DRG), and positively charged L-lysine units at the ends (KKKK-GRD-ARGSV↓NITEGE-DRG-KKKK). This peptide formed nanoparticles with alginate by ionotropic gelation. Exposure to an infection-related protease led to the degradation of particles and the subsequent release of encapsulated drugs.^[15] Ramezani et al. have synthesized a triblock copolymer based on polyethylene glycol (PEG) linked to polylactide (PLA) via a synthetic peptide with the sequence PVGLIG.^[16] This PEG-*b*-PVGLIG-*b*-PLA block copolymer was able to form self-assembled polymersomes and to encapsulate 7-ethyl-10-hydroxycamptothecin, an antitumor agent, with a high efficiency. The peptide sequence PVGLIG can be selectively cleaved by the tumor-associated matrix metalloproteinase 2 enzyme leading to a 7 folds higher release compared to an polymersome without peptide linker.^[16] In extension of this concept and taking advantage of the superior drug encapsulation of polymersomes, it might be interesting to incorporate a cleavable peptide sequence into an amphiphilic graft copolymer. Thus, a chitosan-g[peptide-poly- ϵ -caprolactone] was synthesized and self-assembled into polymeric vesicles employing the solvent shift method (see **Figure 1**). The hydrophobic polycaprolactone side chains were linked to the hydrophilic chitosan backbone via enzyme-cleavable peptide linker. The synthetic route involved the functionalization of chitosan with maleimide groups and the preparation of polycaprolactone with alkyne end-groups (see **Figure 2**). A peptide functionalized with a thiol group on one side and an azide group on the other side was used as linker, employing thiol-ene click-chemistry and azide-alkyne Huisgen cycloaddition, respectively.

2. Experimental Section

2.1. Materials

Medium molecular weight Chitosan (CS) (degree of deacetylation = 75–85%, $M_w = 190\,000\text{--}310\,000\text{ g mol}^{-1}$), ϵ -caprolactone, tin (II)-2-ethylhexanoate, 1-ethyl-(3-dimethylaminopropyl carbodiimide) hydrochloride (EDC), and hydroxybenzotriazole monohydrate (HOBt) were purchased from Sigma Aldrich. 3-Maleimidopropionic acid (Mal) and copper(I)bromide were purchased from Alfa Aesar. Azide-poly-L-lysine-thiol as a linear

heterobifunctional poly(L-lysine) with an azide and a thiol group on the PLL ends with $n = 20$ lysine units was purchased from Nanosoft Polymers.

2.2. Synthesis of Chitosan-Maleimide (CS-Mal) (Figure 2, Step 1)

CS-Mal was synthesized according to Matsumoto et al. (Figure 2, Step 1).^[17] Briefly, CS (100 mg) and HOBt (91 mg, 0.5 mmol) were dissolved in 3 mL of ultrapure water and stirred overnight. To the CS solution, 33 mL of dimethyl sulfoxide (DMSO) and a variable amount of 3-maleimidopropionic acid were added. Subsequently, EDC (114 mg, 0.5 mmol) in HCl solution (200 μL , pH = 4–5) was added, and the mixture was stirred for 24 h at room temperature. Finally, the reaction mixture was dialyzed against a solution containing $10 \times 10^{-3}\text{ M}$ HCl, 1 wt% NaCl, and a solution with $10 \times 10^{-3}\text{ M}$ HCl. Subsequently the solution was lyophilized to obtain CS-Mal. ¹H-NMR and Fourier transform infrared (FT-IR) spectroscopy were used to characterize CS-Mal.

¹H-NMR (400 MHz, D₂O) δ [ppm] = 2.00–2.08 (m, 3H, CH₃ of GlcNAc); 3.07–3.24 (m, 1H, CH of GlcN); 3.43–4.09 (m, 5H, CH on chitosan backbone); 4.52–5.01 (m, 1H, O–CH–O); 6.85 (s, 2H, HC=CH).

FT-IR [cm^{-1}]: 3248 (O–H); 2875 (C–H); 1704 (C=C); 1645 (C=O); 1556 (N–H); 1422 (CH–OH), 1699 (C=C), 1045 cm^{-1} (C–O).

2.3. Synthesis of Propargyl-Terminated Poly- ϵ -Caprolactone (PCL-Alkyne) (Figure 2, Step 2)

PCL-alkyne was synthesized via a general procedure for ring-opening polymerization of poly(ϵ -caprolactone):^[18] ϵ -caprolactone, propargyl alcohol, and Tin (II)-2-ethylhexanoate were dissolved in dry toluene. The solution was stirred at 110 °C under dry nitrogen gas for 24 h. The solution was then cooled down to room temperature. After cooling, tetrahydrofuran was added to dilute the solution. Finally, PCL-alkyne was precipitated in a significant excess of methanol, filtered, washed with methanol, and dried in a vacuum oven at 40 °C for 48 h. Molecular weight was calculated to $M_n = 5755\text{ g mol}^{-1}$ by the integration of terminal proton of CH₂ at 3.62 ppm and the corresponding protons of CH₂-groups in the chain at 4.03 ppm.

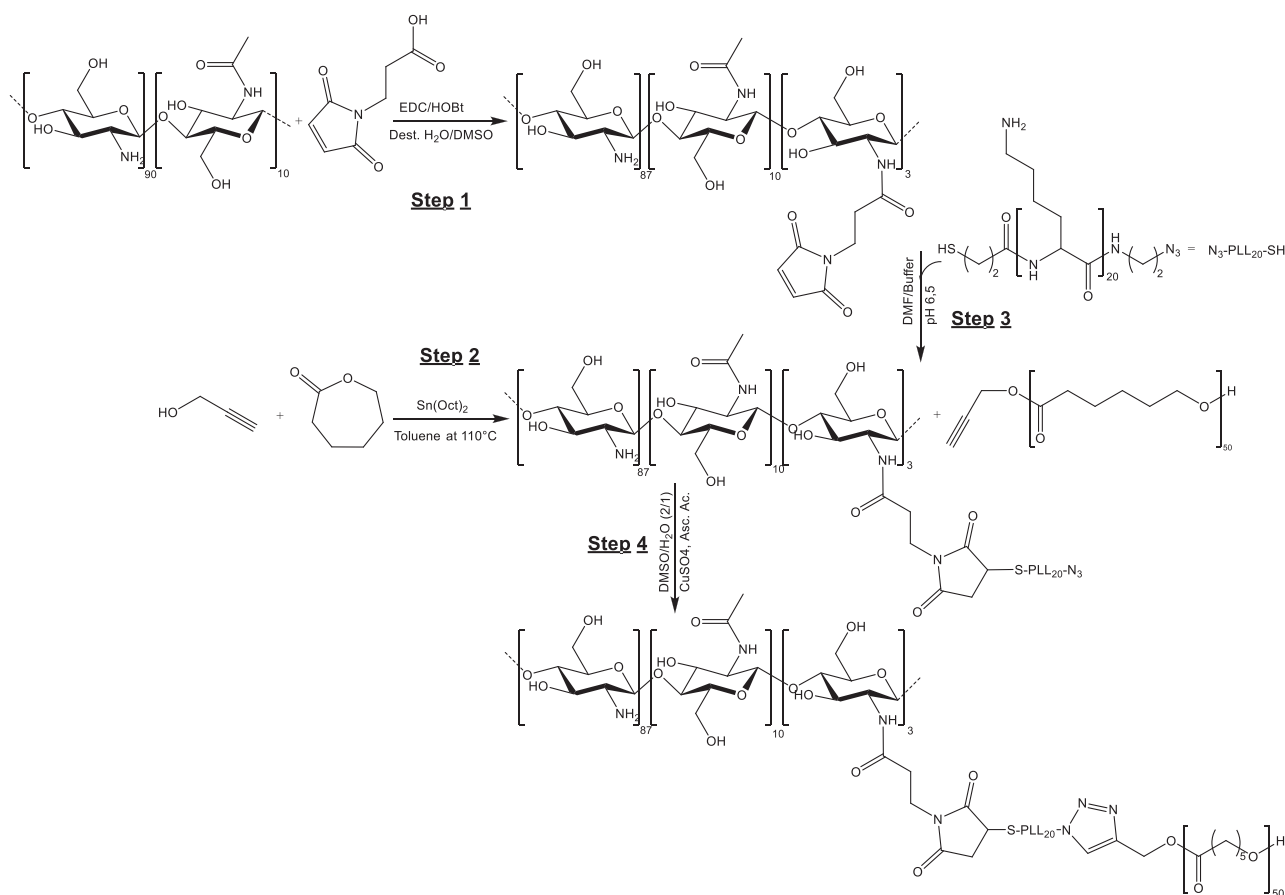


Figure 2. Synthesis pathway for chitosan-g-[poly-L-lysine-*b*- ϵ -caprolactone].

¹H-NMR and FT-IR spectroscopy were used to characterize PCL-alkyne.

¹H-NMR (400 MHz, CDCl₃) δ [ppm] = 1.36 (m, 90H, CH₂ on PCL backbone); 1.62 (m, 180H, CH₂ on PCL backbone); 2.27 (m, 90H, CH₂C=O on PCL backbone); 2.45 (s, 1H, CH₂-C \equiv CH); 3.62 (t, 2H, CH₂OH); 4.03 (m, 88H, CH₂O on PCL backbone); 4.65 (s, 2H, CH₂-C \equiv CH).

FT-IR [cm⁻¹]: 3265 (C \equiv C-H); 2944 (C-H); 2855 (C-H); 2098 (C \equiv C); 1721 (C=O); 1469 (C-H); 1238 ((C=O)-O); 1171 cm⁻¹ (C-O-C).

2.4. Synthesis of CS-[poly-L-lysine₂₀-N₃] (CS-[PLL₂₀-N₃]) (Figure 2, Step 3)

CS-Mal with a DS of 3% or 5% and a molar equivalent amount of azido-poly-L-lysine₂₀-Cys were dissolved in a mixture of DMF and phosphate buffered saline (ratio: 1/6) with a final pH of 6.5. After the complete dissolution, the mixture was stirred for 24 h at room temperature. Subsequently, the solution was dialyzed against a solution containing 10 \times 10⁻³ M HCl and 1 wt% NaCl, and 10 \times 10⁻³ M HCl solution. Finally, the solution was lyophilized to obtain CS-[PLL₂₀-N₃].

¹H-NMR (400 MHz, D₂O) δ [ppm] = 2.00–2.08 (m, 3H, CH₃ of GlcNAc); 3.07–3.24 (m, 1H, CH of GlcN); 3.43–4.09 (m, 5H,

CH on chitosan backbone); 4.52–5.01 (m, 1H, O-CH-O); poly-L-lysine 4.31 (m, 1H, CH); 2.98 (t, 2H, CH₂); 1.7 (m, 4H, -CH₂); 1.43 (m, 2H, CH₂).

FT-IR relevant peaks [cm⁻³]: 2121 (-N₃)

2.5. Synthesis of Chitosan-g-[PLL-poly- ϵ -caprolactone] (CS-[PLL-PCL]) (Figure 2, Step 4)

PCL-alkyne (1.79 μ mol) and CS-([PLL₂₀-N₃])_{3%} (0.01 g) were dissolved in a mixture of 2 mL DMSO and 1 mL H₂O at 37 $^{\circ}$ C. After dissolution, a mixture of CuSO₄·5H₂O (3.57 μ mol) and Ascorbic acid (8.93 μ mol) were added to the reaction mixture. The solution was stirred overnight at 37 $^{\circ}$ C. Finally, the resulting copolymer was dialyzed against THF in order to remove unreacted PCL-alkyne, against a saturated aqueous solution of ethylenediaminetetraacetic acid (EDTA) disodium salt, 10 \times 10⁻³ M HCl, 1 wt% NaCl solution, and against 10 \times 10⁻³ M HCl solution. After lyophilization, the copolymer was obtained.

¹H-NMR (400 MHz, D₂O/DMSO) δ [ppm] = PCL backbone: 1.30 (m, CH₂ on PCL backbone); 1.54 (m, 2 \times CH₂ on PCL backbone); 2.27 (m, CH₂C=O on PCL backbone); 3.99 (m, CH₂); Chitosan backbone: 1.87 (m, 3H, -CH₃ of GlcNAc); 2.93 (m, 1H, CH of GlcN); 3.73–3.86 (m, 5H, CH on chitosan backbone),

4.95 (m, 1H, O—CH—O); poly-L-lysine: 4.24 (m, 1H, CH); 2.80 (m, 2H, CH₂); 1.64 (m, 4H, CH₂); 1.41 (m, 2H, CH₂).

FT-IR [cm⁻³] relevant peaks: Chitosan component: 3287 (O—H); 2876 (C—H); 1646 (C=O); 1526 (N—H); 1045 cm⁻¹ (C—O); PCL component: 2928 (C—H); 2862 (C—H); 1724 (C=O); 1466 (C—H); 1239 ((C=O)—O); 1175 (C—O).

2.6. Polymersome Formation

For polymersome formation, 1 mg mL⁻¹ CS-graft-copolymer was dissolved in a mixture of H₂O or 63 × 10⁻³ M sodium phosphate buffer pH of 7.6 and DMSO (ratio: 1/20) at 37 °C. After dissolution, the solution was dialyzed (molecular weight cut-off 14,000 g mol⁻¹) three times against deionized H₂O or 63 × 10⁻³ M sodium phosphate buffer pH of 7.6. After 15 h, the solution turned turbid, and the polymersomes were obtained. Then, particle size, zeta potential, and stability measurements were carried out using a Zetasizer Nano ZS from Malvern Instruments (Malvern, UK). Disposable sizing cuvettes (DTS0012) and disposable folded capillary cell (DTS1070) were used for size/zeta potential measurements. Malvern Zetasizer Software Version 7.03 was used for data evaluation. Cryo-SEM images were used to inspect the shape and morphology of polymersomes using a HITACHI S-4800 instrument (Chiyode, Japan).

2.7 Spray Coating of Titanium Substrates

Titanium plates, with a diameter of 1.1 cm (medical grade 4), provided by BRASSELER (Lemgo, Germany) were used as substrates for polymer films. Before being coated, the Ti plates were polished with a Phoenix 4000 device (BUEHLER, Esslingen, Germany) using the following protocol. The plates were treated with SiC abrasive paper (P400) and polished with a polycrystalline diamond suspension (9 μm) on an Ultrapad polish paper and a MestMet colloidal silica polishing suspension (0.02–0.06 μm) on ChemoMet paper. BUEHLER provided all suspensions and papers used for the above procedure. Once polished, the plates were cleaned by ultrasonification, in water followed by dichloromethane, acetone, methanol, and, finally, in MilliQ water. Afterwards, the plates were dried under nitrogen flow and stored in the refrigerator. Prior to each coating process, the plates were thermally treated overnight in order to obtain the desired negatively charged titanium oxide layer. The titanium substrates were then spray-coated for 180 seconds with an airbrush Aztek A470 from Testors (Vernon Hills, IL, USA), depositing ≈20 μL of the polymer-some dispersion with a concentration of 1 mg mL⁻¹. Subsequently, the Ti plates were washed with 0.1 % acetic acid (AcOH) and H₂O in an ultrasonic bath for 15 min. Subsequently, the plates were dried under nitrogen flow. Ellipsometry was used to determine the coating thickness using a Multiskop from Optrel (Sinzing, Germany) in the ellipsometry mode. Uncoated titanium plates were used as a reference. Data were collected in the χ, γ -mode at 70° as mean value of 16 data points in total. Evaluation of the data was carried out using the software Elli Version 3.2 from Optrel.

2.8. Stability and Degradation Experiments with Polymersomes and Coatings

The degradation studies of the coatings on the Ti plates were carried out by the incubation in trypsin (4 μg mL⁻¹) or chitosanase (5 μg mL⁻¹) containing solution. The tests have been performed in distilled water at pH between 5.6 and 5.8. The solutions were renewed daily to ensure degradation capability of trypsin. Before each thickness measurement, the samples were washed with 0.1 % acetic acid (AcOH) and H₂O solutions in an ultrasonic bath for 15 min and dried under nitrogen flow.

The degradation of the polymersomes was investigated by the addition of trypsin or chitosanase to the dispersion. The tests have been performed in 63 × 10⁻³ M sodium phosphate buffer pH of 7.6 and distilled water (pH = 5.6–5.8). Briefly, 1 mL polymersome suspension were filled in a sizing cell. Trypsin or chitosanase solution was added in order to obtain final concentrations of 4 and 5 μg mL⁻¹, respectively. The degradation process was then monitored via consecutive size measurements using the Zetasizer Nano ZS.

2.9. Cryo Scanning Electron Microscopy

For the morphological characterization the samples were cooled by plunging into nitrogen slush at atmospheric pressure and freeze fractured at -180 °C and etched for 60 s at -98 °C. After sputtering with platinum in the GATAN Alto 2500 cryo preparation chamber the samples were transferred into the Hitachi S-4800 microscope (Chiyode, Japan).

2.10. Characterization

A FT-IR Equinox 55 instrument (BRUKER, Billerica, Massachusetts, USA) equipped with a mercury cadmium telluride detector, and an attenuated total reflection accessory with a zinc selenide crystal from Harrick Scientific Products (Pleasantville, United States) was used to perform FT-IR spectroscopy. The following conditions were used: wavelength range between 4000 and 550 cm⁻¹, 10 kHz and 32 scans per sample. The evaluation was carried out with the software OPUS from BRUKER (version 4.0.24).

¹H-NMR measurements were performed with an AV III 400 instrument, (Bruker, Billerica, USA), with magnetic field strength of 400 MHz. The deuterated solvents were purchased from Deutero (Kastellaun, Germany). The evaluation was carried out with the analytical software MestReNova from MESTRELAB (Paris, France).

3. Results and Discussion

The graft polymer chitosan-g-[poly-L-lysine-*b*-ε-caprolactone] (CS-g-[PLL-PCL]) was synthesized in four steps (Figure 2). In the first step, maleimide groups were introduced as side chains at the chitosan backbone with different degrees of substitution (DS) via a reaction between carboxylic acid of *N*-maleoyl-β-alanine and the amine function of chitosan (Figure 2, Step 1).^[17]

In FT-IR spectra a signal assigned to the amide I group at 1645 cm^{-1} was found, which increased with increasing DS (see Figure S5 in the Supporting Information). By contrast, the signal at 1556 cm^{-1} , representing primary amine bending, decreased with increasing substitution. These findings were regarded as a result of the reaction between amines of chitosan and the carboxylic acid resulting in amide bonds. Furthermore, a signal at 1704 cm^{-1} was found, which is the characteristic vibrational frequency of $\text{C}=\text{C}$ bending originating from the maleimide functions. The protons of the *N*-acetyl-D-glucosamine and the D-glucosamine unit of chitosan as well as two proton signals of the maleimide double bond (6.85 ppm) were noticed in the $^1\text{H-NMR}$ spectra of maleimide substituted chitosan (see Figure S1 in the Supporting Information). The DS was calculated from the $^1\text{H-NMR}$ spectra, using the ratio of maleimide protons at 6.85 ppm and the signal at 2.00–2.08 ppm which represents 3 protons of the chitosan backbone. The degree of acetylation of unmodified chitosan was measured by $^1\text{H-NMR}$ and was found to be 10%.

Propargyl-terminated poly- ϵ -caprolactone was synthesized by ring opening polymerization of ϵ -caprolactone (ϵ -CL) by using Tin(II) 2-ethylhexanoate ($\text{Sn}(\text{oct})_2$) as catalyst and propargyl alcohol as initiator.^[18] The molar ratio of ϵ -CL, propargyl alcohol, and $\text{Sn}(\text{oct})_2$ was set to 83:2:1. $^1\text{H-NMR}$ spectra were used to confirm the presence of both alkyne function and PCL backbone signals (see Figure S2 in the Supporting Information). The peaks at 4.65 and 2.45 ppm represent $\text{HC}\equiv\text{C}$ – and $\text{C}-\text{CH}_2$ – protons of the propargyl function, respectively. The protons at 1.36, 1.62, 2.27, 4.03, and 3.62 ppm represent PCL backbone protons. Furthermore, FT-IR analysis was employed to confirm the structure. The characteristic vibrational bands of PCL-alkyne appear at 1721 cm^{-1} ($\text{C}=\text{O}$ stretching), 1238 cm^{-1} ($\text{C}-\text{O}-\text{C}$ asymmetric stretching) and 1171 cm^{-1} (symmetric $\text{C}-\text{O}-\text{C}$ stretching) (see Figure S5 in the Supporting Information). The signal at 3265 cm^{-1} ($\text{H}-\text{C}\equiv\text{C}$ – stretching) highlighted the end-terminal alkyne function. The average molecular weight $M_n = 5755\text{ g mol}^{-1}$ was calculated from the $^1\text{H-NMR}$ spectrum. The calculation was based on the integration of proton peaks of CH from the alkyne function at 4.65 ppm and PCL backbone at 4.03 ppm. The theoretical M_n calculated from the ratio of initiator and monomer was $M_{n,\text{theor}} = 6770\text{ g mol}^{-1}$.

Propargyl-terminated poly- ϵ -caprolactone was synthesized by ring opening polymerization of ϵ -caprolactone (ϵ -CL) by using Tin(II) 2-ethylhexanoate ($\text{Sn}(\text{oct})_2$) as catalyst and propargyl alcohol as initiator.^[18] The molar ratio of ϵ -CL, propargyl alcohol, and $\text{Sn}(\text{oct})_2$ was set to 83:2:1. $^1\text{H-NMR}$ spectra were used to confirm the presence of both alkyne function and PCL backbone signals (see Figure S2 in the Supporting Information). The peaks at 4.65 and 2.45 ppm represent $\text{HC}\equiv\text{C}$ – and $\text{C}-\text{CH}_2$ – protons of the propargyl function, respectively. The protons at 1.36, 1.62, 2.27, 4.03, and 3.62 ppm represent PCL backbone protons. Furthermore, FT-IR analysis was employed to confirm the structure. The characteristic vibrational bands of PCL-alkyne appear at 1721 cm^{-1} ($\text{C}=\text{O}$ stretching), 1238 cm^{-1} ($\text{C}-\text{O}-\text{C}$ asymmetric stretching) and 1171 cm^{-1} (symmetric $\text{C}-\text{O}-\text{C}$ stretching) (see Figure S5 in the Supporting Information). The signal at 3265 cm^{-1} ($\text{H}-\text{C}\equiv\text{C}$ – stretching) highlighted the end-terminal alkyne function. The average molecular weight $M_n = 5755\text{ g mol}^{-1}$ was calculated

from the $^1\text{H-NMR}$ spectrum. The calculation was based on the integration of proton peaks of CH from the alkyne function at 4.65 ppm and PCL backbone at 4.03 ppm. The theoretical M_n calculated from the ratio of initiator and monomer was $M_{n,\text{theor}} = 6770\text{ g mol}^{-1}$.

Thiol-ene click-chemistry and azide-alkyne Huisgen cycloaddition were used to link chitosan and poly- ϵ -caprolactone chains, respectively, through the peptide linker. For this purpose, a peptide end-functionalized with a thiol on one side and an azide at the other end was used. The ligation between the thiol end-functionalized peptide and the maleimide-functionalized chitosan (Figure 2, Step 3) was carried out as thiol-ene click chemistry, also known as Thiol-Michael addition. Generally, the reaction between thiol and a double bond can be initiated with different catalysts, such as organometallics, bases, Lewis acids, metals, and nucleophiles.^[19] Light,^[20] heat,^[21] or radical initiators^[21] are also used to initiate the reaction by generating a thiol radical capable to undergo the reaction.^[22] A uniqueness of the maleimide function is the presence of carbonyl groups in *cis*-conformation coupled with ring-strain/bond-angle distortion, which increases the reactivity of the double bond toward the thiol function with the help of the solvent. In fact, it is common for such reactions to be performed in the presence of, e.g., DMF as solvent and catalyst.^[23] Solvents such as DMSO and DMF possess a high dielectric constant, which promotes the spontaneous dissociation of thiol into nucleophilic thiolate anion. Subsequently, the thiolate is able to react with the double bond of the maleimide function.^[24] Nevertheless, DMSO is also known to catalyze undesired disulfide bond formation;^[25] therefore, DMF was chosen as the optimal solvent for this synthesis. In addition to solvent choice, pH plays a crucial role. The reaction between a maleimide and thiol function specifically occurs at physiological pH (6.5–7.5), generating a stable thioester bond. At a pH above 8.0, the reactivity between the double bond and amines of chitosan is significantly increased, which leads to side reactions.^[26,27] The reaction was checked by $^1\text{H-NMR}$ spectroscopy, which showed the disappearance of the maleimide double bond protons at 6.85 ppm; these protons are involved in the reaction with thiolate. New signals at 1.43, 1.70, 2.98, and 4.31 ppm characteristic for the protons of the PLL backbone indicated the presence of the peptide (see Figure S3 in the Supporting Information). The FT-IR analysis was also used to confirm the reaction and to demonstrate the appearance of a vibrational band at 2126 cm^{-1} , which is characteristic for the azide function grafted on the chitosan (see Figure S5 in the Supporting Information). The DS was calculated from the $^1\text{H-NMR}$ -spectra, using the ratio of PLL protons at 4.52–5.01 ppm and the signal at 2.00–2.08 ppm which represents 3 protons of chitosan backbone.

Finally, CS-g-[PLL-PCL] was synthesized by 1,3-Huisgen dipolar cycloaddition, also known as the “copper click reaction”. The reaction occurs between the azide function of the peptide already grafted onto CS and the alkyne function of the PCL. The reaction was catalyzed by $\text{CuSO}_4 \cdot 5\text{H}_2\text{O}$ and sodium ascorbic acid as agent to reduce unreactive Cu(II) to Cu(I). For purification a dialysis against tetrahydrofuran (THF) was carried out to remove unreacted PCL, followed by dialysis against a saturated aqueous solution of EDTA to remove copper.^[28] The solution was subsequently dialyzed against water to remove the

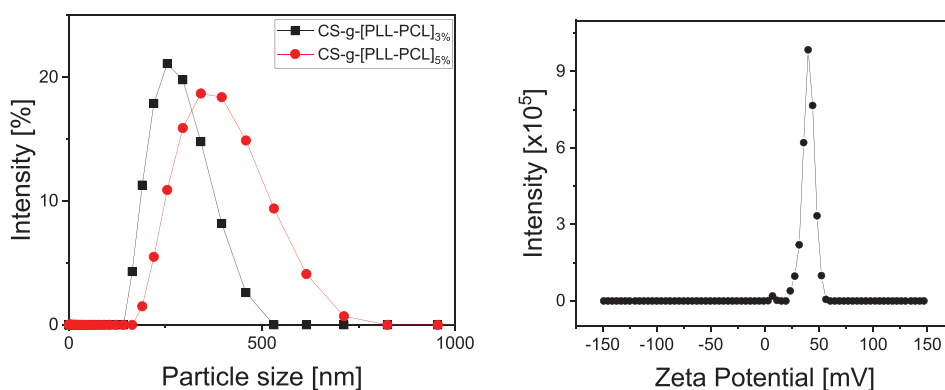


Figure 3. DLS size distribution of CS-g-[PLL-PCL]_{5%} and CS-g-[PLL-PCL]_{3%} and zeta potential of CS-g-[PLL-PCL]_{3%} polymersomes in distilled H₂O at rt.

complex formed by copper and EDTA. ¹H-NMR spectroscopy, operated at a temperature of 50 °C to ensure the solubility of the copolymer was used to validate the synthesis of CS-g-[PLL-PCL] (see Figure S4 in the Supporting Information). The peaks at 4.24, 2.80, 1.64, and 1.41 ppm are characteristic for PLL protons in DMSO/H₂O mixture. The peaks at 4.95, 3.86–3.73, 2.93, 1.87 ppm are originating from the chitosan backbone. Finally, the peaks at 3.99, 2.27, 1.54, and 1.30 ppm are characteristic for the PCL backbone protons. In addition, the disappearance of the peak at 2121 cm⁻¹ in the IR-spectrum confirmed the consumption of the azide groups (see Figure S5 in the Supporting Information). The chitosan and PLL backbones can be characterized by the band at 1646 cm⁻¹ (C=O stretching of amide I) and strong bands at 3287, 3340 cm⁻¹ that correspond to N–H and O–H stretching. The bands at 1045 cm⁻¹ correspond to C–O stretching of chitosan. The DS was calculated from the ¹H-NMR spectra, using the ratio of PCL protons at 3.99 ppm and 3 protons of chitosan backbone at 1.87 ppm.

After the successful synthesis of amphiphilic graft copolymer, its self-assembly into polymersomes and their degradability by enzymes were studied. Polymersome formation depends on different factors. One main factor is the hydrophilic to hydrophobic ratio. Studies have suggested that a hydrophilic mass fraction from 20% to 45% is a unifying rule for achieving self-assembly into polymersomes.^[29] Based on this rule, two graft copolymers, with mass fractions in or near this range, were synthesized: CS-g-[PLL-PCL]_{3%} with a hydrophilic mass fraction of 50%, and CS-g-[PLL-PCL]_{5%} with hydrophilic mass fraction of 40%, respectively. As described in the experimental part, the polymersomes were generated by the solvent shift method to induce the self-assembly process. Briefly, this method includes dissolving the copolymer in DMSO/H₂O and slowly removing the DMSO by dialysis against H₂O. During this process, the hydrophobic and hydrophilic parts self-assembled into polymersomes through hydrophobic interactions. DLS was used to measure the size of the polymersomes.

Both graftpolymers gave polymersomes with a monomodal size distribution. Compared with polymersomes prepared from CS-g-[PLL-PCL]_{3%}, with a mean size of 258 nm, CS-g-[PLL-PCL]_{5%} gave larger particles with an average size of 427 nm (Figure 3). The increase can be explained by the relation between shape, weight fraction of the hydrophilic part, Mw, and the interaction strength of the hydrophobic fraction with water.

Furthermore, polymersomes can be predicted according to the equation $p = v/a \cdot l$, where “*p*” is the packing parameter, “*v*” is the volume of the hydrophobic chains, “*a*” is the optimal area of the head group, and “*l*” is the length of the hydrophobic tail.^[30] Therefore, the ratio between hydrophilic and hydrophobic fraction affects the size/shape of polymersomes. With the increase in size also the polydispersity index (PDI) increased from 0.129 for 3% to 0.351 for 5%. In drug delivery applications using carriers with PDI of 0.3 and below is considered to be acceptable and indicates an homogeneous population of particles.^[31] Therefore, CS-g-[PLL-PCL]_{3%} was used in the following experiments. Measurements of the zeta-potential (see Figure 3) indicated a positive potential of $\approx +41 \pm 4.3$ mV. This is an indication that ammonium groups of chitosan are oriented toward the outer water phase as represented in Figure 4-II.

Cryo-SEM micrographs (see Figure 4-I) revealed well-defined core-shell structures for the polymersomes with a size range centered around 300 nm, which is consistent with the size measured by DLS.

For testing the colloidal stability (Figure 5), the particle size was monitored via DLS while polymersomes were incubated in H₂O at pH 5.6. The tests were performed at 37 °C. Compared with room temperature measurements (Figure 3), CS-g-[PLL-PCL]_{3%} polymersomes at 37 °C exhibited an increased initial size (Figure 5, time = 0), which is a consequence of measuring at a higher temperature. During the incubation period, the size decreased slightly at a rate of ≈ 0.43 nm h⁻¹ (Figure 5). This is attributed to some sedimentation of larger, probably aggregated particles during the DLS measurements. However, this is not attributed to a chemical degradation of the graft-polymers, as coatings prepared from the particle suspensions are very stable (vide infra). Similar tests were performed in a 63×10^{-3} M sodium phosphate buffer, pH 7.6 to observe the stability of polymersomes at physiological pH. Again some decrease in particle size was observed after 6 days, which is very similar to the situation at pH 5.6 (see Fig 6).

The degradability of the well-defined polymersomes was studied by incubating them with different enzymes in water, namely trypsin, which is able to cleave poly-L-lysine^[32] and chitosanase, which endohydrolyzes β -1,4-linkages of partially acetylated chitosan.^[33] As described in the experimental part, the polymersome dispersion was treated with a 4 μ g mL⁻¹ trypsin solution and a 5 μ g mL⁻¹ chitosanase solution. DLS

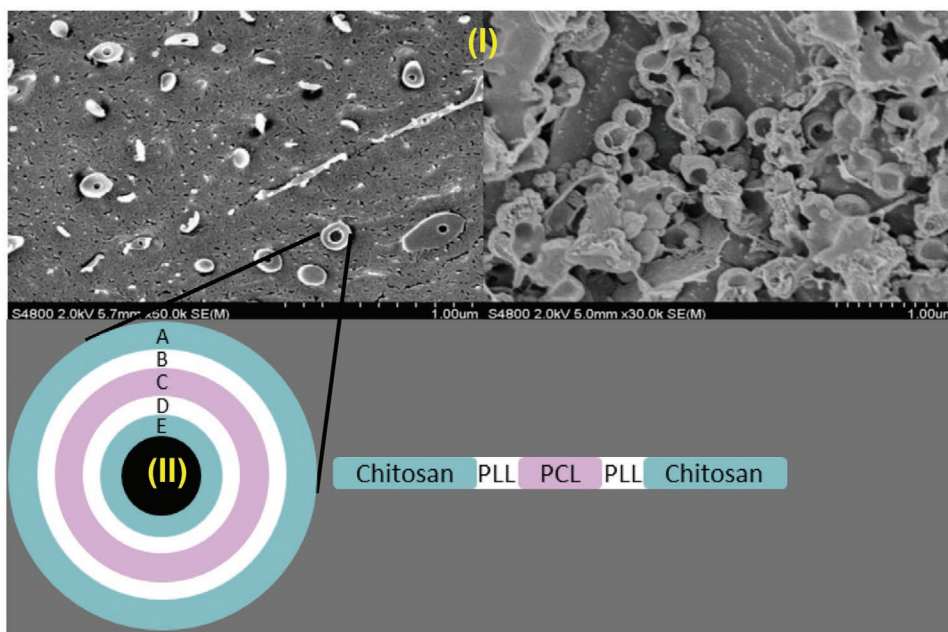


Figure 4. SEM micrographs of cryo-fractured surface of I) CS-g-[PLL-PCL]_{3%} polymersomes solution in ultrapure water and II) schematic representation of polymersomes with A/E, chitosan; B/D, poly-L-lysine; C, poly-ε-caprolactone.

measurements were used to determine particle sizes before and after 6 days incubation.

Incubation tests (**Figure 6B**) with trypsin indicated no relevant variation in particle size compared to the incubation in water (**Figure 6A**) or buffer (**Figure 6C**). In fact, in experiments A and C without trypsin (**Figure 6**), the same small decrease in size was observed after 6 days, which was probably due to the sedimentation of larger polymersome aggregates. Thus polymersomes were stable against trypsin. However, incubation with chitosanase (**Figure 7A**) resulted in a significant increase in particle size, while for incubation without chitosanase, again a slight decrease was observed (**Figure 7B**). The somewhat counterintuitive increase in particle size due to the degradation can

be explained by the reduction in the hydrophilic part (chitosan) hydrolyzed by chitosanase, which consequently results in an increase in the hydrophobic fraction in the graft copolymer. Since shape and size of the polymersomes depend on the weight fraction of the hydrophilic part, M_w , and the interaction strength of the hydrophobic fraction with water.^[30] As a consequence a change in the hydrophilic part formed due to the degradation of the chitosan results in changes of the aggregation or a variation in shape, which both induce a change in particle size.

A further stability test was carried out with films on titanium substrates prepared by spray-coating a dispersion of

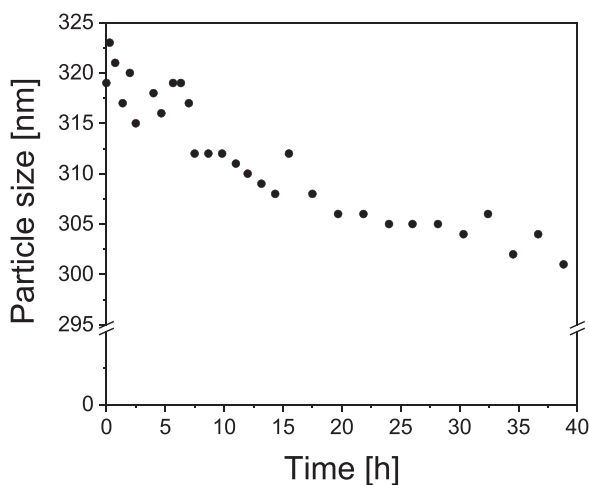


Figure 5. Particle size of CS-g-[PLL-PCL]_{3%} incubated in ultrapure H₂O monitored for 40 h at 37 °C.

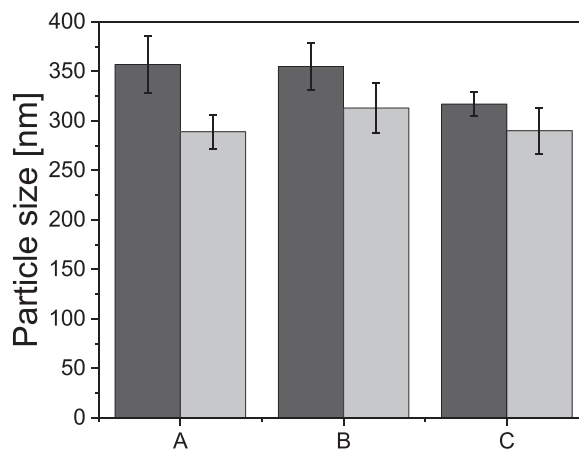


Figure 6. Particle size before ■ and after □ incubation of CS-g-[PLL-PCL]_{3%} polymersome at 37 °C for 6 days in different media. A) H₂O pH = 5.6; B) H₂O, pH = 5.6 with trypsin (4 µg mL⁻¹), and C: 63 × 10⁻³ M sodium phosphate buffer pH = 7.6.

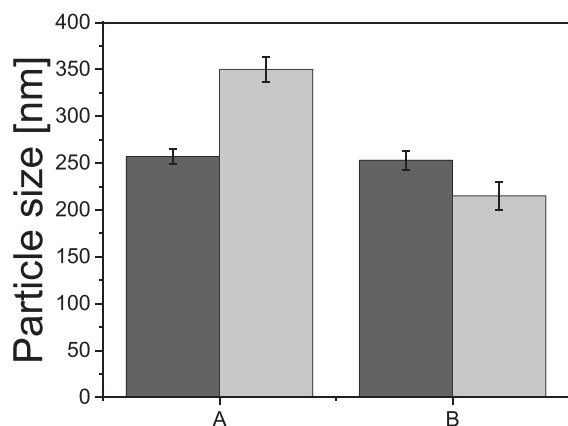


Figure 7. Particle size before ■ and after 72 h incubation □ of CS-g-[PLL-PCL]_{3%} polymersome at rt. A) with chitosanase (5 μg mL⁻¹) and B) without.

polymersomes CS-g-[PLL-PCL]_{3%}. After drying, the films were incubated in water and in water with chitosanase or trypsin, respectively. After certain incubation times the dry thickness of the films was determined via ellipsometry. **Figure 8** depicts the variation in layer thickness during incubation with either water (blue curve), water with chitosanase (5 μg/mL; red curve) or with trypsin (4 μg mL⁻¹; black curve) for 11 days. The solutions were refreshed daily to ensure the degradation capability of enzymes.

After 11 days of incubation with just water or a trypsin solution no significant decrease in dry thickness was noticed; these observations are an indication for a stable coating. However after incubation in a chitosanase solution, a decrease in the layer thickness by 52% was observed (Figure 8). In contrast to the situation for the polymersomes in dispersion were an increase in particle size was observed (see Figure 7), here indeed a decrease in film thickness is detected. This is because the degradation of the chitosan chains results in less material being bound to the surface. A similar behavior

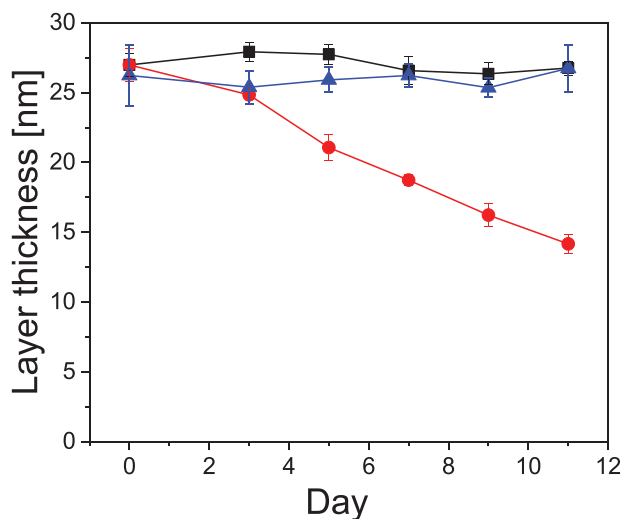


Figure 8. Layer thickness of CS-g-[PLL-PCL]_{3%} coated on Ti plates during incubation with water containing chitosanase ● (5 μg mL⁻¹), trypsin ■ (4 μg mL⁻¹), and without enzyme ▲ at 37 °C.

(particle growth and film thickness reduction) has been observed before for chitosan/tripolyphosphate nanoparticles and coatings, respectively.^[34]

The degradation of the polymersomes via a specific cleavage of the PLL-linker by trypsin was not confirmed. This might be explained by the difficulty of the enzyme reaching the PLL layer: (Figure 4-II (B) and/or (D)). PLL is located at the border of the polymersome compartments which is between the hydrophobic PCL (C) layer and hydrophilic chitosan (A) and (E) layer (Figure 4-II). For this reason, trypsin must diffuse through the chitosan layers (A) or (C) (Figure 4-II) to reach the substrate (PLL). According to Buck et al. bovine trypsin has an isoelectric point (pI) of 10.5^[35] and thus is positively charged at pH < 7.6, which is the highest pH for the degradation tests. Consequently, the enzyme is subjected to repulsive interactions with the positively charged chitosan. Chitosanase has a similar isoelectric point (pI) of 9.6 and therefore has also a net positive charge at a pH of 5.6.^[36] However, chitosanase was still able to reduce the thickness of a coating prepared with the polymersomes. An explanation for these findings is that chitosan is localized at the surface of the polymersome and is thus easily accessible for enzymes. In conclusion, with the chitosan outer layer, the linker region is not easily accessible for proteases like trypsin. Likewise, the chitosan layer will protect any peptide in the inner compartment from degradation by trypsin or other proteases. The chitosan shell, however, can be enzymatically degraded by specialized enzymes like chitosanase. In humans, due to the lack of chitosanase, chitosan can be very stable depending on the degree of deacetylation.^[37] Therefore, the polymersomes can be used to generate a chitosanase-responsive drug delivery system for example against plant fungal diseases. For instance, Okazaki et al. purified chitosanase produced from the pathogenic plant fungus, *Fusarium solani* f. sp. *phaseoli*.^[38] An infection of the plant by this fungus would lead to the release of chitosanases which can degrade the chitosan based responsive delivery system.

4. Conclusions

A new amphiphilic graft-copolymer based on two biocompatible polymers has been synthesized. CS and PCL were linked via a peptide to form a graft-polymer, which is able to self-assemble into polymersomes using the solvent shift method. These polymersomes were characterized via dynamic light scattering, zeta-potential measurements and cryo-SEM. A relationship between the particle size and the amount of hydrophobic PCL was demonstrated. This might be interesting for optimizing the encapsulation and diffusion rate of encapsulated drugs. Cryo-SEM images highlighted well-defined spherical core-shell structures. The stability of the polypeptide linker against degradation by trypsin was demonstrated for the polymersomes and for coatings prepared therefrom. The stability was attributed to the chitosan layer which cannot be penetrated by the trypsin. However, incubation with chitosanase, known for hydrolysis of chitosan, led to a degradation of the graft-polymer as indicated by increase in particle size for the polymersomes and a reduction of the dry layer thickness of coatings on titanium plates.

Supporting Information

Supporting Information is available from the Wiley Online Library or from the author.

Acknowledgements

This work was supported by the Deutsche Forschungsgemeinschaft DFG (Grant Me1057/18-1). The layout mistakes in the figure legends were corrected on January 15, 2021.

Open access funding enabled and organized by Projekt DEAL.

Conflict of Interest

The authors declare no conflict of interest.

Keywords

chitosan, click chemistry, drug delivery system, enzyme, polymersomes, poly- ϵ -caprolactone

Received: July 23, 2020

Revised: October 15, 2020

Published online: December 2, 2020

- [1] E. Rideau, R. Dimova, P. Schwille, F. R. Wurm, K. Landfester, *Chem. Soc. Rev.* **2018**, 47, 8572.
- [2] K. Rajagopal, D. A. Christian, T. Harada, A. Tian, D. E. Discher, *Int. J. Polym. Sci.* **2010**, 379286.
- [3] T. Anajafi, S. Mallik, *Ther. Delivery* **2015**, 6, 521.
- [4] X. Hu, Y. Zhang, Z. Xie, X. Jing, A. Bellotti, Z. Gu, *Biomacromolecules* **2017**, 18, 649.
- [5] F. Itel, M. Chami, A. Najer, S. Lörcher, D. Wu, I. A. Dinu, W. Meier, *Macromolecules* **2014**, 47, 7588.
- [6] J. Leong, J. Y. Teo, V. K. Aakalu, Y. Y. Yang, H. Kong, *Adv. Healthcare Mater.* **2018**, 7, 1701276.
- [7] R. C. Amos, A. Nazemi, C. V. Bonduelle, E. R. Gillies, *Soft Matter* **2012**, 8, 5947.
- [8] W. Chen, J. Du, *Sci. Rep.* **2013**, 3, 2162.
- [9] F. Liu, V. Kozlovskaya, S. Medipelli, B. Xue, F. Ahmad, M. Saeed, D. Cropek, E. Kharlampieva, *Chem. Mater.* **2015**, 27, 7945.
- [10] C. Nehate, A. Nayal, V. Koul, *ACS Biomater. Sci. Eng.* **2019**, 5, 70.
- [11] Q. Yan, J. Yuan, Z. Cai, Y. Xin, Y. Kang, Y. Yin, *J. Am. Chem. Soc.* **2010**, 132, 9268.
- [12] H. Oliveira, E. Pérez-Andrés, J. Thevenot, O. Sandre, E. Berra, S. Lecommandoux, *J. Controlled Release* **2013**, 169, 165.
- [13] P. S. Kulkarni, M. K. Haldar, R. R. Nahire, P. Katti, A. H. Ambre, W. W. Muhonen, J. B. Shabb, S. K. R. Padi, R. K. Singh, P. P. Borowicz, D. K. Shrivastava, K. S. Katti, K. Reindl, B. Guo, S. Mallik, *Mol. Pharmaceutics* **2014**, 11, 2390.
- [14] B. Law, R. Weissleder, C.-H. Tung, *Biomacromolecules* **2006**, 7, 1261.
- [15] C. Tolle, J. Riedel, C. Mikolai, A. Winkel, M. Stiesch, D. Wirth, H. Menzel, *Biomolecules* **2018**, 8, 103.
- [16] P. Ramezani, K. Abnous, S. M. Taghdisi, M. Zahiri, M. Ramezani, M. Alibolandi, *Colloids Surfaces, B* **2020**, 193, 111135.
- [17] M. Matsumoto, W. Udomsinprasert, P. Laengee, S. Honsawek, K. Patarakul, S. Chirachanchai, *Macromol. Rapid Commun.* **2016**, 37, 1618.
- [18] L. G. Bach, M. R. Islam, X. T. Cao, J. M. Park, K. T. Lim, *J. Alloys Compd.* **2014**, 582, 22.
- [19] D. P. Nair, M. Podgórski, S. Chatani, T. Gong, W. Xi, C. R. Fenoli, C. N. Bowman, *Chem. Mater.* **2014**, 26, 724.
- [20] M. Sangermano, R. Bongiovanni, G. Malucelli, A. Priola, A. Harden, N. Rehnberg, *J. Polym. Sci. A: Polym. Chem.* **2002**, 40, 2583.
- [21] M. Uygun, M. A. Tasdelen, Y. Yagci, *Macromol. Chem. Phys.* **2010**, 211, 103.
- [22] A. Dondoni, A. Marra, *Chem. Soc. Rev.* **2012**, 41, 573.
- [23] H. Kakwere, S. Perrier, *J. Am. Chem. Soc.* **2009**, 131, 1889.
- [24] B. H. Northrop, S. H. Frayne, U. Choudhary, *Polym. Chem.* **2015**, 6, 3415.
- [25] J. P. Tam, C. R. Wu, W. Liu, J. W. Zhang, *J. Am. Chem. Soc.* **1991**, 113, 6657.
- [26] G. T. Hermanson, *Bioconjugate Techniques*, 3. Aufl., Elsevier, Amsterdam **2013**.
- [27] J. S. Nanda, J. R. Lorsch, *Methods Enzymol.* **2014**, 536, 79.
- [28] W. A. R. van Heeswijk, M. J. D. Eenink, J. Feijen, *Synthesis* **1982**, 1982, 744.
- [29] D. E. Discher, A. Eisenberg, *Science* **2002**, 297, 967.
- [30] H. Che, J. C. M. van Hest, *J. Mater. Chem.* **2016**, 4, 4632.
- [31] M. Danaei, M. Dehghankhold, S. Ataei, F. Hasanzadeh Davarani, R. Javanmard, A. Dokhani, S. Khorasani, M. R. Mozafari, *Pharmaceutics* **2018**, 10, 57.
- [32] S. G. Waley, J. Watson, *Biochem. J.* **1953**, 55, 328.
- [33] J. Saito, A. Kita, Y. Higuchi, Y. Nagata, A. Ando, K. Miki, *J. Biol. Chem.* **1999**, 274, 30818.
- [34] S. Sydow, A. Aniol, C. Hadler, H. Menzel, *Biomolecules* **2019**, 9, 573.
- [35] F. F. Buck, A. J. Vithayathil, M. Bier, F. F. Nord, *Arch. Biochem. Biophys.* **1962**, 97, 417.
- [36] J. K. Park, K. Shimono, N. Ochiai, K. Shigeru, M. Kurita, Y. Ohta, K. Tanaka, H. Matsuda, M. Kawamukai, *J. Bacteriol.* **1999**, 181, 6642.
- [37] T. Jiang, R. James, S. G. Kumbar, C. T. Laurencin, in *Natural and Synthetic Biomedical Polymers*, Vol. 5 (Eds: S. G. Kumbar, C. T. Laurencin, M. Deng), Elsevier, Amsterdam **2014**, p. 91.
- [38] M. Shimosaka, M. Nogawa, Y. Ohno, M. Okazaki, *Biosci. Biotechnol. Biochem.* **1993**, 57, 231.